JOURNAL OF AIRCRAFT
Vol. 45, No. 2, March–April 2008

Dynamic Multimode Response of Composite Plates to Sonic Boom and Blast Loadings

Vedat Dogan*
Istanbul Technical University, 34469 Istanbul, Turkey

DOI: 10.2514/1.30196

In this study, the linear and nonlinear displacement responses of an antisymmetric angle-ply composite plate subjected to sonic boom and air blast loadings are addressed. The first-order shear deformation theory is used for the governing equations so that the shear deformations can be taken into account for the responses of moderately thick plates. The von Kármán type of geometric nonlinearities are considered and the rectangular composite plate is assumed to be simply supported on all edges. A multimode Galerkin approach is used to obtain the equation of motion in the time domain, and those equations are solved by a Runge–Kutta fifth-order method. The influences of a large number of parameters are investigated, such as damping ratio, geometric nonlinearity, number of modes, characteristic of the blast, plate geometry, and fiber orientation.

I. Introduction

THE extensive use of laminated composites in the construction of aerospace structures continues to grow. Compared with metallic counterparts, composite plates made with several layers of high-strength lamina experience lower structural weight, and the new developments in manufacturing techniques with more affordable cost render them more attractive for use. Aircraft and spacecraft are typically weight-sensitive structures in which composite materials can be cost effective [1]. However, composites are weak against transverse shear, therefore, shear deformations, particularly for moderately thick plates, need to be incorporated into functional analyses. Linear and nonlinear analyses of composite plates using different theories have been well developed and extensively used [2].

The modern fighter aircraft constructed from laminated composites is likely to be exposed to time-dependent explosive blast or sonic boom loadings on its surfaces during its service life. Librescu and Nosier [3] investigated the dynamic response of symmetrically laminated rectangular composite plates subjected to sonic boom and explosive blast loading using different plate theories (classic and higher-order theories). Dynamic responses of sandwich-type panels to air blast and underwater shock loading are addressed in [4–6]. Geometrically nonlinear sandwich models, anisotropic face sheets, and orthotropic cores are used. Extensive parametric studies are carried out on the structural response. Turkmen and Mecitoglu [7,8] performed the experimental and numerical investigation of nonlinear responses of laminated plates exposed to blast loadings. Kazanci and Mecitoglu [9] examined the nonlinear damped vibrations of composite plates subject to blast loading, and Wei and Dharani [10] used small-deflection and large-deflection theories for a rectangular laminated glazing subject to blast loading. They showed that the negative phase of a blast loading has a significant effect on the dynamic response. Gupta et al. [11] considered the response of a rectangular plate subjected to an explosive blast load. They compared the closed-form solution with the ADINA finite element code, and found excellent agreement for the linear elastic dynamic case. Houlston et al. [12,13] investigated the nonlinear structural response of ship panels to air blast loading by using finite element analysis (ADINA) and experimental results. Beshara [14] scrutinized the modeling of blast loads needed for the structural analysis of above-ground structures. Olson [15] worked on new modeling methods for stiffened plates and cylindrical shells subject to blast loadings.

This paper addresses the nonlinear and linear responses of simply supported antisymmetric angle-ply composite plates to sonic boom and explosive blast loadings. Both thin and moderately thick composite plates are considered and von Kármán-type geometric nonlinearities are assumed. Results are obtained within the first-order shear deformation theory (FSDT), which involves five coupled partial differential equations. The time history of the input is taken as an N-shaped pulse for a sonic boom and as an exponentially decaying pressure for an explosive blast. A multimode Galerkin approach is used to obtain the response in the time domain. A numerical technique is carried out to obtain the displacement response histories for different cases.

II. Equations of Motion

The displacements (u, v, w) for the laminated plate in the first-order shear deformation theory are

$$\begin{aligned} u(x,y,z,t) &= u_0(x,y,t) + z\phi_x(x,y,t) \\ v(x,y,z,t) &= v_0(x,y,t) + z\phi_y(x,y,t) \\ w(x,y,z,t) &= w_0(x,y,t) \end{aligned} \tag{1}$$

where (u_0, v_0, w_0) are the middle surface displacements (i.e., $z = 0$) in the x, y, and z directions, respectively, and ϕ_x and ϕ_y are the rotations of a transverse normal about the y and x axes, respectively. The nonlinear strain-displacement relationships are

$$\{\varepsilon\} = \{\varepsilon^0\} + z\{\varepsilon^1\} \tag{2}$$

$$\begin{Bmatrix} \varepsilon_{xx} \\ \varepsilon_{yy} \\ \gamma_{xy} \end{Bmatrix} = \begin{Bmatrix} \varepsilon^0_{xx} \\ \varepsilon^0_{yy} \\ \gamma^0_{xy} \end{Bmatrix} + z\begin{Bmatrix} \varepsilon^1_{xx} \\ \varepsilon^1_{yy} \\ \gamma^1_{xy} \end{Bmatrix} = \begin{Bmatrix} u_{0,x} + (1/2)(w_{0,x})^2 \\ v_{0,y} + (1/2)(w_{0,y})^2 \\ u_{0,y} + v_{0,x} + w_{0,x}w_{0,y} \end{Bmatrix} + z\begin{Bmatrix} \phi_{x,x} \\ \phi_{y,y} \\ \phi_{x,y} + \phi_{y,x} \end{Bmatrix} \tag{3}$$

$$\begin{Bmatrix} \gamma_{yz} \\ \gamma_{xz} \end{Bmatrix} = \begin{Bmatrix} \gamma^0_{yz} \\ \gamma^0_{xz} \end{Bmatrix} = \begin{Bmatrix} w_{0,y} + \phi_y \\ w_{0,x} + \phi_x \end{Bmatrix} \tag{4}$$

Received 1 February 2007; accepted for publication 6 October 2007.

*Assistant Professor, Department of Aeronautics and Astronautics, Maslak; doganve@itu.edu.tr.

For a composite laminate, the force and moment resultants are

$$\begin{Bmatrix}\{N\}\\ \{M\}\end{Bmatrix}=\begin{bmatrix}[A] & [B]\\ [B] & [D]\end{bmatrix}\begin{Bmatrix}\{\varepsilon^0\}\\ \{\varepsilon^1\}\end{Bmatrix} \tag{5}$$

$$\begin{Bmatrix}Q_y\\ Q_x\end{Bmatrix}=\kappa\begin{bmatrix}A_{44} & A_{45}\\ A_{45} & A_{55}\end{bmatrix}\begin{Bmatrix}\gamma^0_{yz}\\ \gamma^0_{xz}\end{Bmatrix} \tag{6}$$

where

$$(A_{ij},B_{ij},D_{ij})=\int_{-h/2}^{h/2}\bar{Q}^k_{ij}(1,z,z^2)\,\mathrm{d}z \qquad i,j=1,2,6 \tag{7}$$

$$A_{ij}=\int_{-h/2}^{h/2}\bar{Q}^k_{ij}\,\mathrm{d}z \qquad i,j=4,5 \tag{8}$$

where $\bar{Q}^k_{ij}$ are the reduced stiffness coefficients of the kth layer, and h is the total thickness of the plate. Using these relationships and the dynamic version of the principle of virtual work, the nonlinear differential equations of motion for the first-order plate theory are given in Reddy [2]. For an antisymmetric angle-ply laminate

$$A_{16}=0,\quad A_{26}=0,\quad A_{45}=0,\quad B_{11}=0,\quad B_{12}=0,$$
$$B_{22}=0,\quad B_{66}=0,\quad D_{16}=0,\quad D_{26}=0,\quad I_1=0$$

The following boundary conditions for a simply supported laminate (Fig. 1), using the FSDT, are considered as in Reddy [2]:

At $x=0,a$

$$u_0(x,y,t)=w_0(x,y,t)=\phi_y(x,y,t)=N_{xy}(x,y,t)=M_{xx}(x,y,t)=0 \tag{9}$$

At $y=0,b$

$$v_0(x,y,t)=w_0(x,y,t)=\phi_x(x,y,t)=N_{xy}(x,y,t)=M_{yy}(x,y,t)=0 \tag{10}$$

The series solutions which satisfy the boundary conditions are

$$\begin{aligned}
u_0(x,y,t)&=\sum_{m=1}^{M}\sum_{n=1}^{N}U_{mn}(t)\ \sin(\alpha_m x)\ \cos(\beta_n y)\\
v_0(x,y,t)&=\sum_{m=1}^{M}\sum_{n=1}^{N}V_{mn}(t)\ \cos(\alpha_m x)\ \sin(\beta_n y)\\
w_0(x,y,t)&=\sum_{m=1}^{M}\sum_{n=1}^{N}W_{mn}(t)\ \sin(\alpha_m x)\ \sin(\beta_n y)\\
\phi_x(x,y,t)&=\sum_{m=1}^{M}\sum_{n=1}^{N}X_{mn}(t)\ \cos(\alpha_m x)\ \sin(\beta_n y)\\
\phi_y(x,y,t)&=\sum_{m=1}^{M}\sum_{n=1}^{N}Y_{mn}(t)\ \sin(\alpha_m x)\ \cos(\beta_n y)
\end{aligned} \tag{11}$$

where $\alpha_m=m\pi/a$ and $\beta_n=n\pi/b$. Also, M and N are the modal numbers at which the series solution in Eq. (11) is truncated.

Using the series solution of Eq. (11) and a Galerkin approach in the nonlinear partial differential equations of motion, a set of coupled nonlinear ordinary differential equations in time domain is obtained

$$\begin{aligned}
&I_0\ddot{U}_{kl}+I_0c\dot{U}_{kl}+\left(A_{11}\alpha_k^2+A_{66}\beta_l^2\right)U_{kl}+(A_{12}\alpha_k\beta_l+A_{66}\alpha_k\beta_l)V_{kl}\\
&\quad+2B_{16}\alpha_k\beta_lX_{kl}+\left(B_{16}\alpha_k^2+B_{26}\beta_l^2\right)Y_{kl}\\
&\quad+\frac{1}{4}\sum_{mnrs}W_{mn}W_{rs}\Big\{A_{11}{}^{U}\bar{S}^1_{mnrskl}-A_{12}{}^{U}\bar{S}^2_{mnrskl}-A_{66}{}^{U}\bar{S}^3_{mnrskl}\\
&\quad+A_{66}{}^{U}\bar{S}^4_{mnrskl}\Big\}=0
\end{aligned} \tag{12a}$$

$$\begin{aligned}
&I_0\ddot{V}_{kl}+I_0c\dot{V}_{kl}+\left(A_{66}\alpha_k^2+A_{22}\beta_l^2\right)V_{kl}+(A_{66}\alpha_k\beta_l+A_{12}\alpha_k\beta_l)U_{kl}\\
&\quad+\left(B_{16}\alpha_k^2+B_{26}\beta_l^2\right)X_{kl}+2B_{26}\alpha_k\beta_lY_{kl}\\
&\quad+\frac{1}{4}\sum_{mnrs}W_{mn}W_{rs}\Big\{A_{66}{}^{V}\bar{S}^1_{mnrskl}-A_{66}{}^{V}\bar{S}^2_{mnrskl}-A_{12}{}^{V}\bar{S}^3_{mnrskl}\\
&\quad+A_{22}{}^{V}\bar{S}^4_{mnrskl}\Big\}=0
\end{aligned} \tag{12b}$$

$$\begin{aligned}
&I_0\ddot{W}_{kl}+I_0c\dot{W}_{kl}+\kappa\left(A_{55}\alpha_k^2+A_{44}\beta_l^2\right)W_{kl}+\kappa A_{55}\alpha_kX_{kl}\\
&\quad+\kappa A_{44}\beta_lY_{kl}+\frac{1}{4}\sum_{mnrs}W_{rs}\Big\{U_{mn}L^U_{mnrskl}+V_{mn}L^V_{mnrskl}\\
&\quad+X_{mn}L^X_{mnrskl}+Y_{mn}L^Y_{mnrskl}\Big\}\frac{1}{16}\sum_{mnrsij}W_{mn}W_{rs}W_{ij}L^W_{mnrsijkl}\\
&\quad=F_{kl}
\end{aligned} \tag{12c}$$

$$\begin{aligned}
&I_2\ddot{X}_{kl}+I_2c\dot{X}_{kl}+\left(D_{11}\alpha_k^2+D_{66}\beta_l^2+\kappa A_{55}\right)X_{kl}+2B_{16}\alpha_k\beta_lU_{kl}\\
&\quad+\left(B_{16}\alpha_k^2+B_{26}\beta_l^2\right)V_{kl}+\kappa A_{55}\alpha_kW_{kl}+(D_{12}\alpha_k\beta_l\\
&\quad+D_{66}\alpha_k\beta_l)Y_{kl}+\frac{1}{4}\sum_{mnrs}W_{mn}W_{rs}\Big\{B_{16}{}^{X}\bar{S}^1_{mnrskl}-2B_{16}{}^{X}\bar{S}^2_{mnrskl}\\
&\quad+B_{26}{}^{X}\bar{S}^3_{mnrskl}\Big\}=0
\end{aligned} \tag{12d}$$

$$\begin{aligned}
&I_2\ddot{Y}_{kl}+I_2c\dot{Y}_{kl}+\left(D_{22}\beta_l^2+D_{66}\alpha_k^2+\kappa A_{44}\right)Y_{kl}\\
&\quad+\left(B_{16}\alpha_k^2+B_{26}\beta_l^2\right)U_{kl}+2B_{26}\alpha_k\beta_lV_{kl}+\kappa A_{44}\beta_lW_{kl}\\
&\quad+(D_{12}\alpha_k\beta_l+D_{66}\alpha_k\beta_l)X_{kl}+\frac{1}{4}\sum_{mnrs}W_{mn}W_{rs}\Big\{B_{16}{}^{Y}\bar{S}^1_{mnrskl}\\
&\quad-2B_{26}{}^{Y}\bar{S}^2_{mnrskl}+B_{26}{}^{Y}\bar{S}^3_{mnrskl}\Big\}=0
\end{aligned} \tag{12e}$$

where

$$L^U_{mnrskl}=A_{11}{}^{W}\bar{S}^1_{mnrskl}+A_{66}\left({}^{W}\bar{S}^6_{mnrskl}+{}^{W}\bar{S}^{11}_{mnrskl}\right)+A_{12}{}^{W}\bar{S}^{16}_{mnrskl} \tag{13a}$$

$$L^V_{mnrskl}=A_{12}{}^{W}\bar{S}^2_{mnrskl}+A_{66}\left({}^{W}\bar{S}^7_{mnrskl}+{}^{W}\bar{S}^{12}_{mnrskl}\right)+A_{22}{}^{W}\bar{S}^{17}_{mnrskl} \tag{13b}$$

$$L^X_{mnrskl}=B_{16}\left({}^{W}\bar{S}^3_{mnrskl}+{}^{W}\bar{S}^8_{mnrskl}+{}^{W}\bar{S}^{13}_{mnrskl}\right)+B_{26}{}^{W}\bar{S}^{18}_{mnrskl} \tag{13c}$$

$$L^Y_{mnrskl}=B_{16}{}^{W}\bar{S}^4_{mnrskl}+B_{26}\left({}^{W}\bar{S}^9_{mnrskl}+{}^{W}\bar{S}^{14}_{mnrskl}+{}^{W}\bar{S}^{19}_{mnrskl}\right) \tag{13d}$$

$$\begin{aligned}
L^W_{mnrsijkl}&=A_{11}{}^{W}\bar{Z}^1_{mnrsijkl}-A_{12}\left({}^{W}\bar{Z}^2_{mnrsijkl}+{}^{W}\bar{Z}^5_{mnrsijkl}\right)\\
&\quad-A_{66}\left({}^{W}\bar{Z}^3_{mnrsijkl}+{}^{W}\bar{Z}^4_{mnrsijkl}\right)+A_{22}{}^{W}\bar{Z}^6_{mnrsijkl}
\end{aligned} \tag{13e}$$

where the coefficients ${}^{U,V,X,Y}\bar{S}^{1,2,3,4}_{mnrskl}$, ${}^{W}\bar{S}^{1,2,\ldots,19}_{mnrskl}$, and ${}^{W}\bar{Z}^{1,2,\ldots,6}_{mnrsijkl}$ are given in the Appendix.

I_0, I_2 are the mass inertias defined as

$$(I_0, I_2) = \int_{-h/2}^{h/2} (1, z^2)\rho^k \, dz \tag{14}$$

Also, κ is the shear correction factor, c is the viscous damping coefficient, and ρ^k is the mass density of the kth layer.

The generalized force $F_{kl}(t)$ in Eq. (12) is

$$F_{kl}(t) = \int_0^a \int_0^b p(x, y, t) \sin(\alpha_k) \sin(\beta_l) \, dx \, dy \tag{15}$$

To solve the coupled nonlinear equations of motion Eq. (12), the time histories of generalized forces $F_{kl}(t)$ are required. The generalized forces $F_{kl}(t)$ are obtained for the sonic boom and explosive blast loadings which are described in the next section.

III. Explosive Blast and Sonic Boom Loadings

If the blast source is distant enough from the plate and the dimensions of the plate are small, the detonation of an explosive can generate a uniformly distributed pressure on the plate. The blast overpressure can be written in terms of the modified Friedlander exponential decay equation as [3,11,14]

$$p(x, y, t) = p(t) = p_m(1 - t/t_p)e^{-\alpha t/t_p} \tag{16}$$

where both negative and positive phases of the blast are included. In Eq. (16), t_p is the positive phase duration of the impulse measured from time of arrival of the blast at the plate surface, p_m is the peak reflected pressure in excess of the ambient, α is the decay parameter, and t is the elapsed time.

The sonic boom loadings which result from the far-field overpressure produced by a supersonic flight of an aircraft can be expressed as [3,6]

$$p(x, y, t) = p(t) = p_m(1 - t/t_p) \{H(t) - H(t - rt_p)\} \tag{17}$$

where p_m and t_p have the same meaning as in the blast loading, and r is the shock pulse length factor. $H(t)$ is the Heaviside step function ($H(t) = 1$ for $t \geq 0$ and $H(t) = 0$ for $t < 0$).

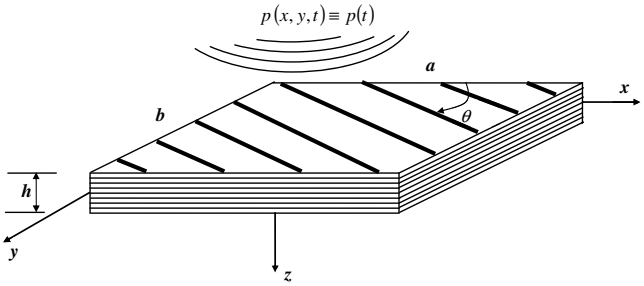

Fig. 1 Laminate geometry and coordinate system.

IV. Numerical Results and Discussion

Antisymmetric angle-ply laminates with eight layers of equal thickness are considered in this section. A stacking sequence with $(\theta/-\theta)_4$, where $\theta = 30$ deg is the ply angle, is considered (Fig. 1). It is assumed that each layer has the following material properties: $E_1 = 132.38$ GPa, $E_2 = 10.76$ GPa, $G_{12} = 5.65$ GPa, $G_{23} = 3.61$ GPa, $\nu_{12} = 0.24$, $\rho = 1390$ kg/m^3, where E, ν, ρ, and G are the Young's modulus, the Poisson's ratio, the mass density, and the shear modulus, respectively. Subscripts denote the material coordinates: 1 is taken to be the fiber direction, 2 is transverse to the fiber direction in the plane of lamina, and 3 is perpendicular to the plane of the lamina. The shear correction factor is taken to be $\kappa = 5/6$. Square laminates with dimension $a = b = 0.3$ m are investigated. Transverse displacement responses are computed at the center of the plate (i.e., $x = a/2$, $y = b/2$).

The damping coefficients in Eq. (12) are taken as

$$c = 2\xi_{kl}\omega_{kl} \tag{18}$$

where ω_{kl} are the natural frequencies of linear vibrations of the composite plate, and the modal damping coefficients are assumed to be

$$\xi_{kl} = \xi_{11}\omega_{11}/\omega_{kl} \quad \text{with} \quad \xi_{11} = 0.05 \qquad \text{(unless otherwise stated)} \tag{19}$$

Two types of antisymmetric angle-ply laminated composite plates are considered in the numerical illustrations. 1) The first plate is a thin laminate ($a/h = 100$). 2) The second plate is a moderately thick laminate ($a/h = 15$).

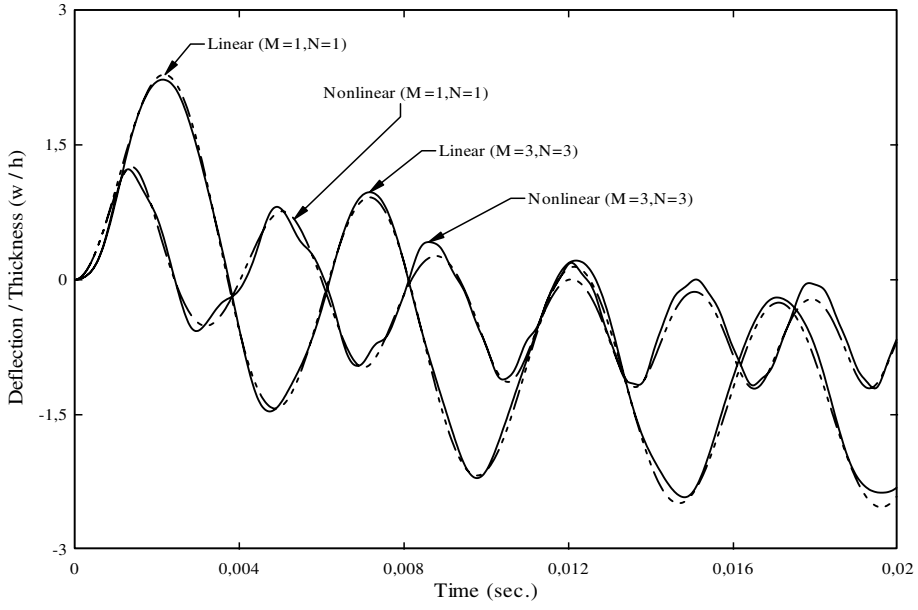

Fig. 2 Linear and nonlinear deflection response histories for the first mode and first nine modes ($a/h = 100$).

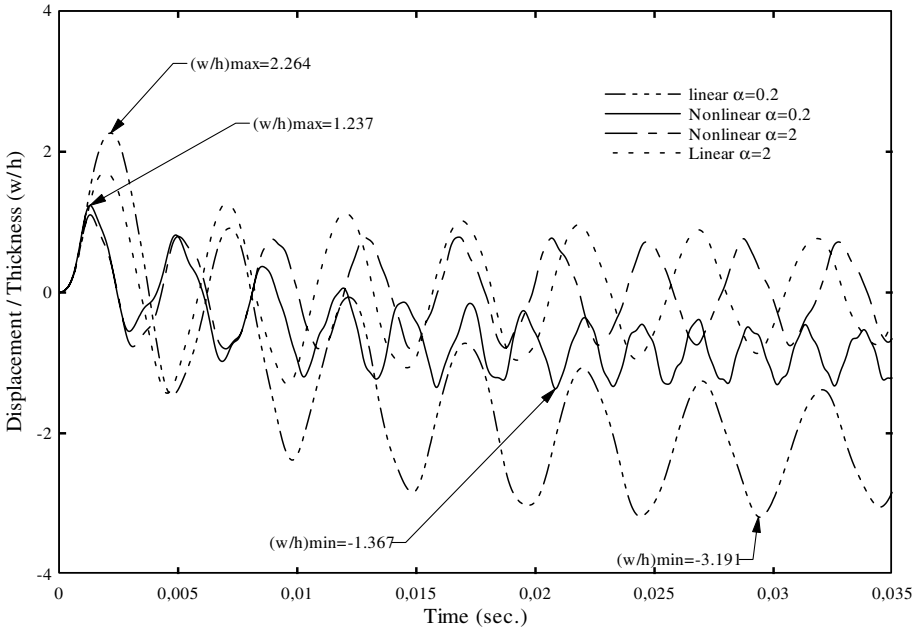

Fig. 3 Response time histories for two values of the parameter α ($M = 3, N = 3$).

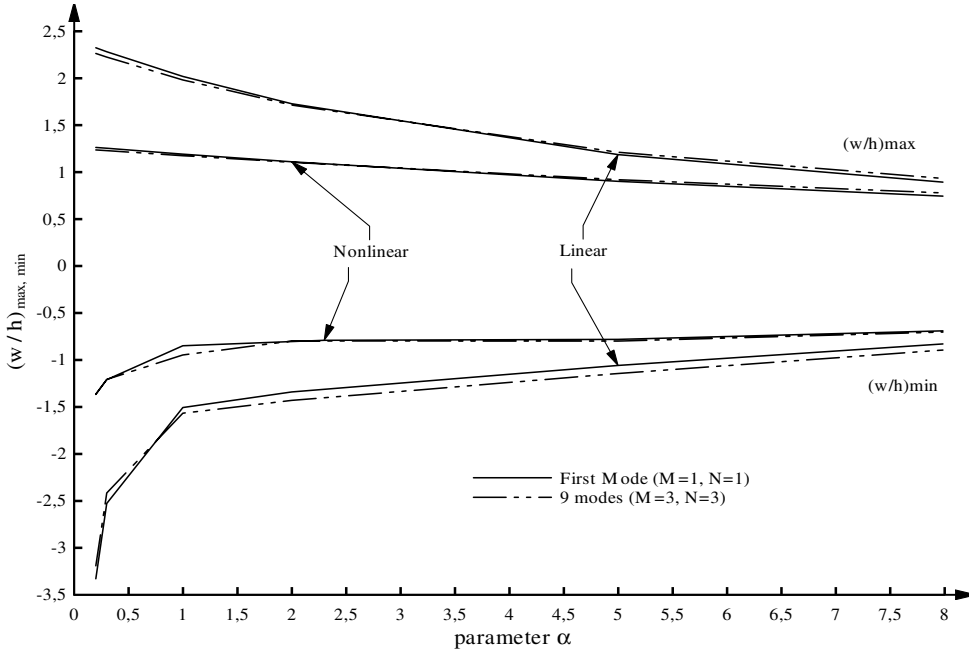

Fig. 4 Maximum/minimum values of dimensionless deflection vs various values of the parameter α.

1) Thin laminate: $a = b = 0.3$ m, $a/h = 100$ ($h = 3$ mm)

$p_m = 20$ kPa, $t_p = 0.005$ s, $\alpha = 0.3$ (unless otherwise stated)

The linear and nonlinear transverse displacement response histories of thin laminate to this explosive blast load are shown in Fig. 2. The dimensionless peak transverse displacement for the linear response is about 81% higher than the dimensionless nonlinear response of 1.24. The time of occurrence of the peak nonlinear response is 0.0013 s as opposed to 0.0021 s for the linear response, indicating a time delay of 62% in attaining the peak values when the nonlinearity effects are not included. Development of membrane forces causes the amplitude and period of the nonlinear response to decrease. A multimode response involving the first nine modes ($M = 3,\ N = 3$) is compared with the fundamental first-mode response ($M = 1, N = 1$). It is obvious that contributions from the higher modes are rather small.

The dimensionless deflection responses of the linear and nonlinear vibrations for two values of the decay parameter α are plotted in Fig. 3. The maximum (positive peak) and minimum (negative peak) values of linear and nonlinear responses for $\alpha = 0.2$ are pointed out in Fig. 3. Indeed, much more insight can be gained from plots of peak values $[(w/h)_{\max}$ and $(w/h)_{\min}]$ vs the parameter α. Figure 4 shows that with the increase of the parameter α, lower amplitudes of the deflection are obtained. The linear response overestimates the dimensionless peak displacement for all the values of α, particularly for $\alpha \leq 1$.

Figure 5 compares the multimode nonlinear deflection responses by using the damping factor $\xi(\equiv \xi_{11})$ as a parameter. The results reveal that the increased damping tends to reduce amplitudes as time increases, as expected. However, the effect of damping at the first

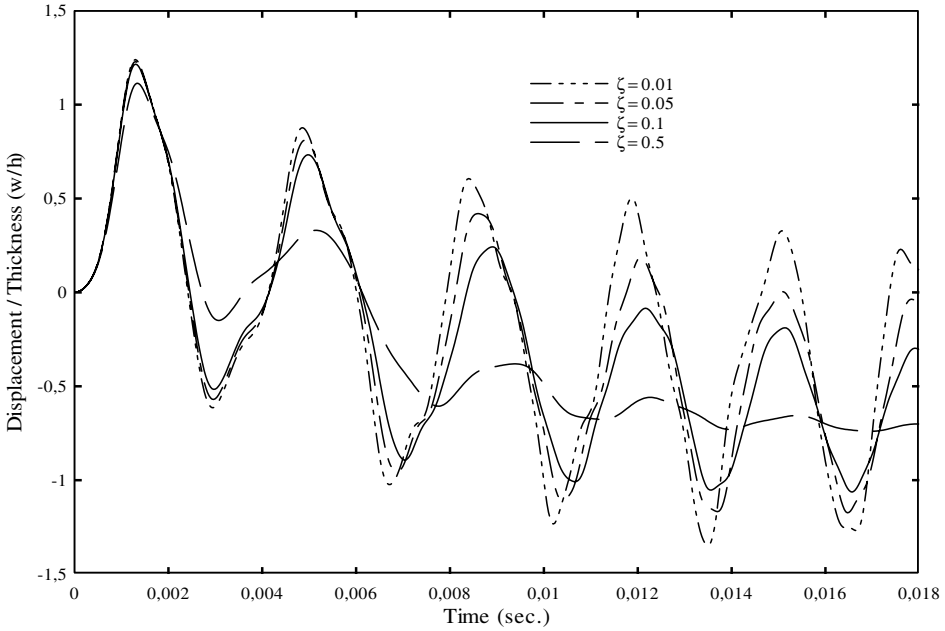

Fig. 5 Effects of the damping on the nonlinear response ($M = 3, N = 3$).

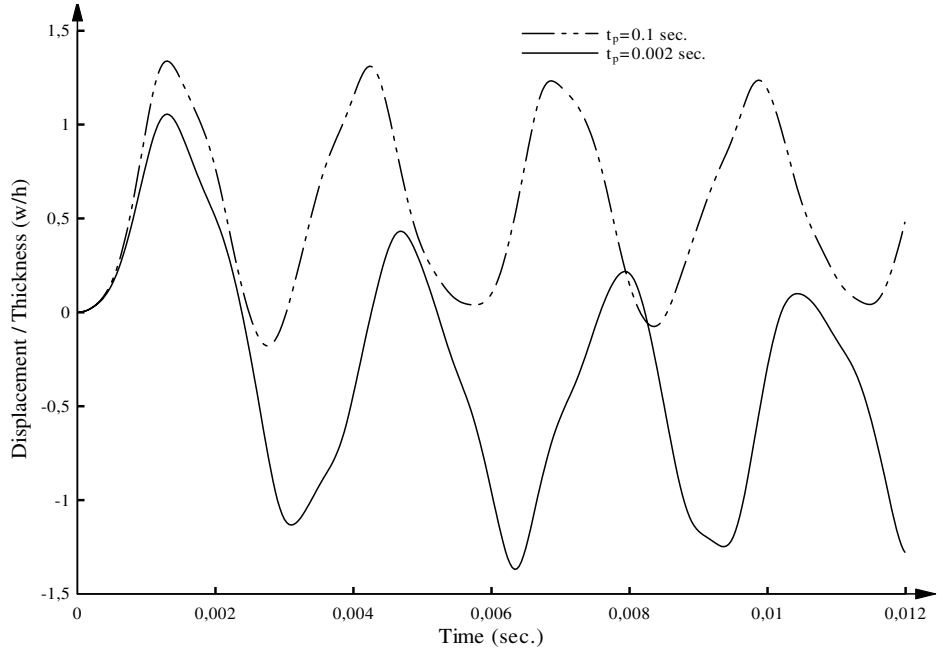

Fig. 6 Effects of the time duration t_p on the nonlinear response for the thin plate ($M = 3, N = 3$).

response peak is quite small. The dimensionless peak transverse displacement for the damping ratio $\xi = 0.5$ is only 9% lower than that for the damping ratio $\xi = 0.01$.

In Fig. 6, the implication of the positive phase duration t_p of the blast load is displayed. It can be seen that for a large value of the positive duration ($t_p = 0.1$ s), the dimensionless peak deflection response of 1.34 occurs at $t = 0.0013$ s, whereas, on the other hand, for a short value of the positive duration ($t_p = 0.002$ s), the dimensionless peak response of -1.37 occurs at $t = 0.0063$ s. It indicates that the response to the blast load is very sensitive to the positive phase duration t_p.

The dimensionless maximum (peak) and minimum (valley) values of linear and nonlinear deflection responses for different ply angles are given in Table 1. Contributions from higher modes are small for all ply angles. The results reveal that $\theta = 45$ deg is the most favorable ply angle for the multimode response because it provides the lowest deflection of the plate.

In Fig. 7, the linear and nonlinear dimensionless deflection response histories to the sonic boom pulse with $r = 2$ are shown. Responses follow the pulse in the forced motion region and then suddenly fluctuate about the zero mean value with decaying amplitude in the free motion region. For the present case, the dimensionless peak transverse displacements for both the linear and nonlinear responses occur at the beginning of the free motion region.

2) Thick laminate: $a = b = 0.3$ m, $a/h = 15$ ($h = 20$ mm)

$p_m = 10^4$ kPa, $t_p = 0.005$ s, $\alpha = 0.3$ (unless otherwise stated)

Figure 8 is the counterpart of Fig. 2 for the case of the thick laminate exposed to a high level of an explosive blast load. Similar

Table 1 Linear and nonlinear dimensionless deflection peak (max) $(w/h)_{max}$ and valley (min) $(w/h)_{min}$ values for different ply angles (thin laminate, $a/h = 100$)

Ply angles, θ	10 deg		20 deg		30 deg		40 deg		45 deg	
	Peak	Valley	Peak	Valley	Peak	Valley	Peak	Valley	Peak	Valley
Linear ($M = 1, N = 1$)	2.955	−3.465	2.599	−2.941	2.281	−2.527	2.112	−2.311	2.090	−2.283
Nonlinear ($M = 1, N = 1$)	1.216	−1.164	1.232	−1.183	1.254	−1.209	1.270	−1.239	1.273	−1.232
Linear ($M = 3, N = 3$)	2.871	−3.336	2.528	−2.812	2.225	−2.416	2.090	−2.212	2.085	−2.209
Nonlinear ($M = 3, N = 3$)	1.234	−1.177	1.240	−1.202	1.229	−1.207	1.206	−1.181	1.201	−1.158

conclusions are reached in this case, however, differences between linear and nonlinear responses for the thick plate are much less than those for the thin plate. Similarly, Figs. 9 and 10 are the counterparts of Figs. 3 and 6, respectively, for the case of the thick laminate. The effects of the variation of the parameters α and t_p on the thick laminate response are similar to those on the thin plate response. Table 2 is the counterpart of Table 1 for the case of thick laminates exposed to an explosive blast load. The results reveal that $\theta = 45$ deg for the multimode response is again the most favorable ply angle.

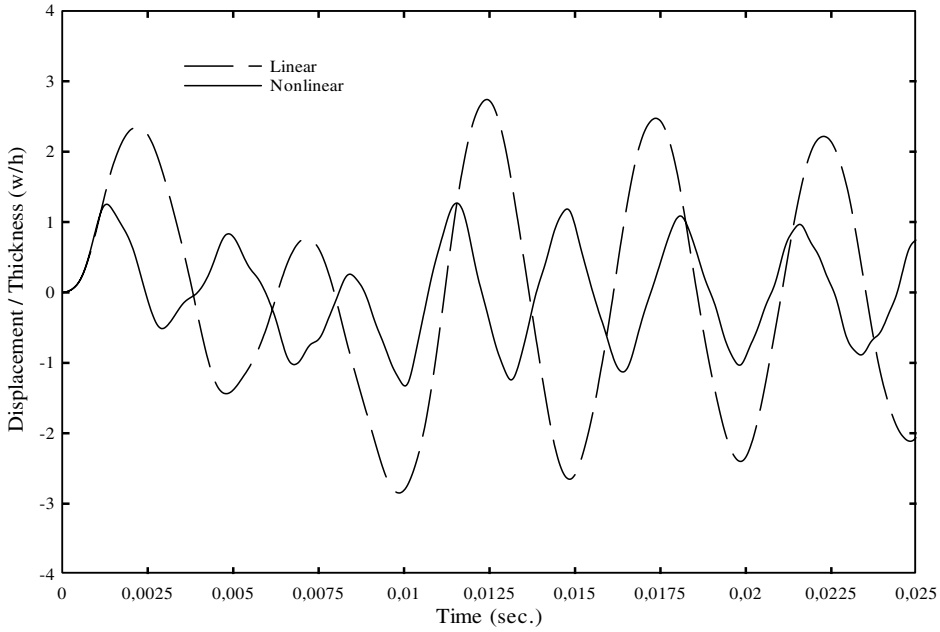

Fig. 7 Deflection time histories due to sonic boom ($a/h = 100$), ($M = 3, N = 3$).

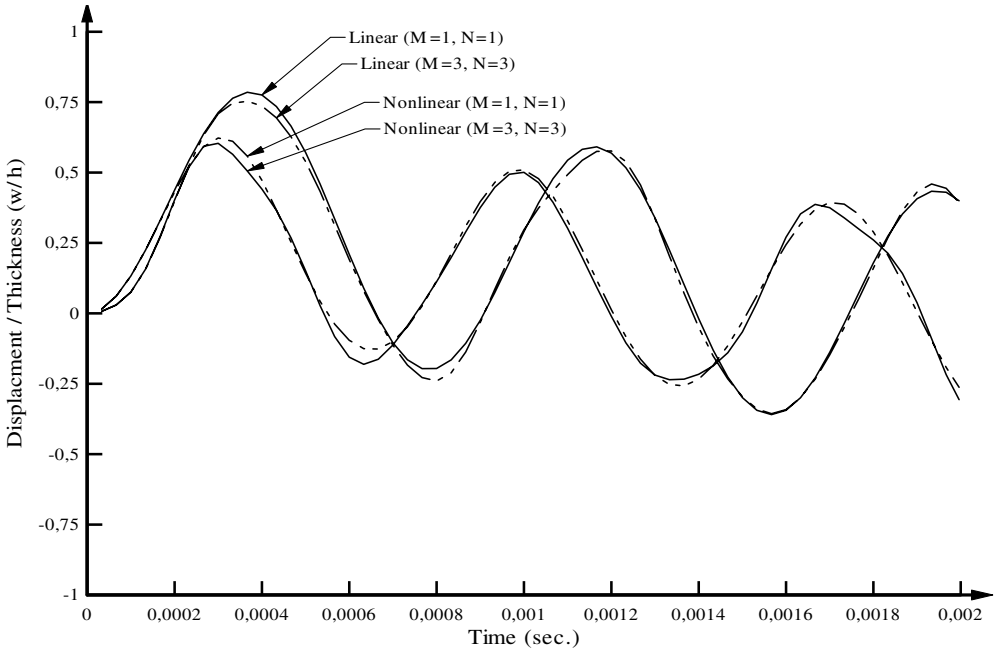

Fig. 8 Linear and nonlinear deflection time histories for the first mode and first nine modes ($a/h = 15$).

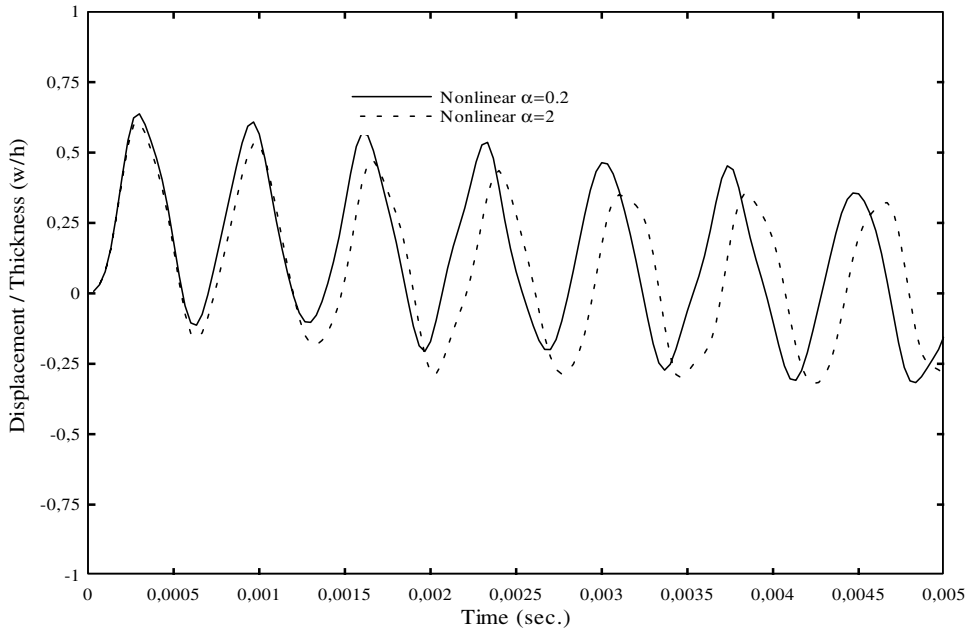

Fig. 9 Nonlinear deflection time histories for two values of the parameter α ($M = 3, N = 3$).

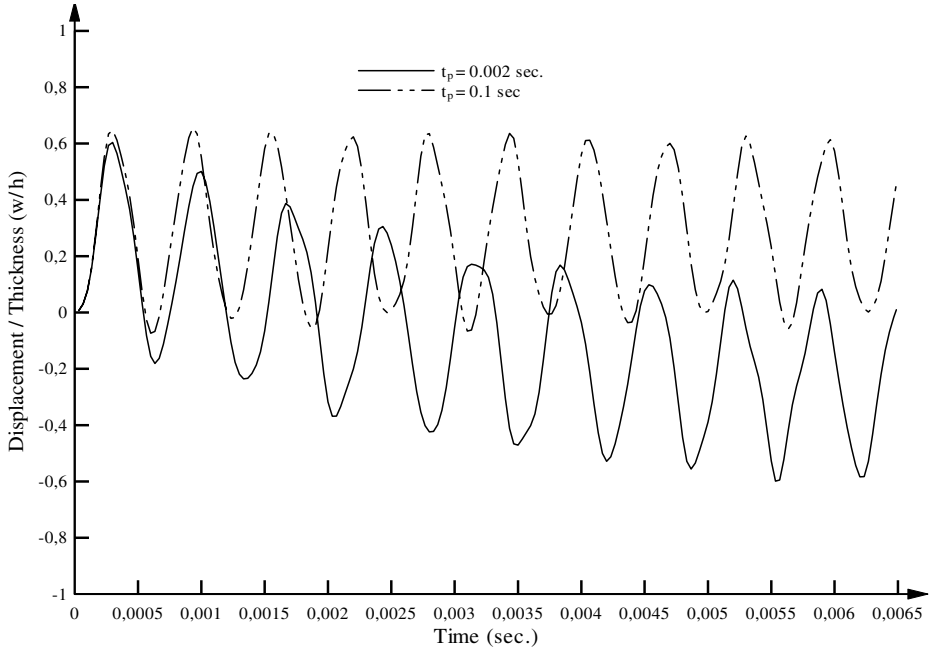

Fig. 10 Effects of the time duration t_p on the nonlinear deflection for the thick plate ($M = 3, N = 3$).

Figure 11 is the counterpart of Fig. 7 for the case of thick laminate subjected to the sonic boom pulse. Unlike the thin laminate case, maximum dimensionless deflections occur in the forced motion region.

Figure 12 displays the absolute maximum/minimum dimensionless deflections $(w/h)_{\max,\min}$ under various peak reflected pressures p_m. Both thin laminates and moderately thick laminates are considered, and the range of nonlinear influence for each plate is

Table 2 Linear and nonlinear deflection peak (max) $(w/h)_{\max}$ and valley (min) $(w/h)_{\min}$ values for different ply angles (thick laminate, $a/h = 15$)

Ply angles, θ	10 deg		20 deg		30 deg		40 deg		45 deg	
	Peak	Valley	Peak	Valley	Peak	Valley	Peak	Valley	Peak	Valley
Linear ($M = 1, N = 1$)	1.134	−0.959	0.979	−0.825	0.849	−0.713	0.786	−0.656	0.778	−0.649
Nonlinear ($M = 1, N = 1$)	0.692	−0.604	0.674	−0.583	0.653	−0.562	0.638	−0.547	0.636	−0.545
Linear ($M = 3, N = 3$)	1.065	−0.942	0.927	−0.807	0.811	−0.689	0.764	−0.646	0.765	−0.631
Nonlinear ($M = 3, N = 3$)	0.700	−0.612	0.670	−0.583	0.631	−0.564	0.607	−0.530	0.607	−0.526

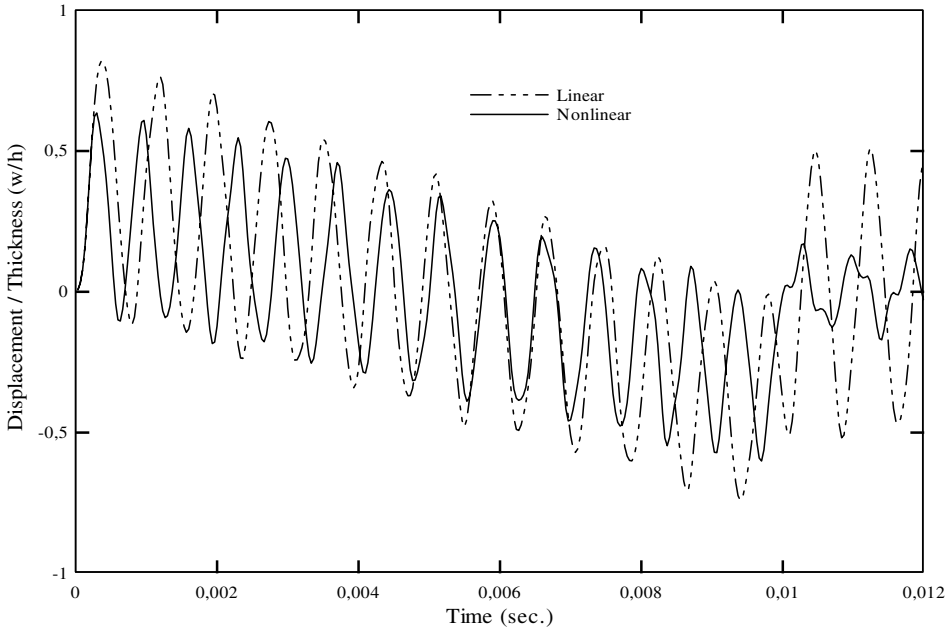

Fig. 11 Deflection time history to sonic boom for the first nine modes ($a/h = 15$).

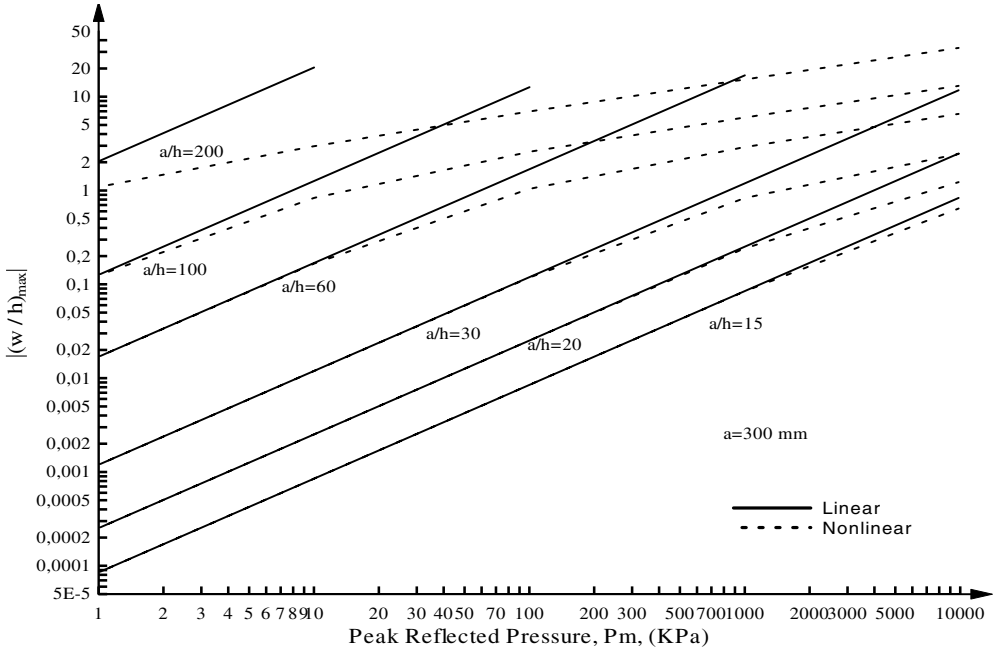

Fig. 12 Linear and nonlinear maximum dimensionless deflections vs peak reflected pressure p_m of blast loadings for various laminates.

realized. The difference between the linear and nonlinear responses is thus due only to large transverse displacement effects. Figure 12 shows that, for deflections on the order of plate thickness, the plates become significantly stiffer due to development of membrane forces.

V. Conclusions

An analytical study of the nonlinear and linear deflection responses of antisymmetric angle-ply composite plates exposed to a sonic boom and an explosive blast loading is presented. Results are obtained within the first-order shear deformation theory. The effects of the various parameters such as α, t_p, and ξ are considered. Results indicate that the larger the parameter α, the smaller the deflection response peaks obtained for both thick and thin laminates. The effect of the parameter t_p on the responses is strong for both loadings. The effect of the damping on the deflection amplitudes is found to be significant as time increases, but the magnitude of the first deflection peak seems to be the same for all values of damping. The ply angles for the investigated laminates play a small role, but $\theta = 45$ is still the most favorable angle for both thin and thick laminates. The ranges of nonlinear and linear normalized deflections vs overpressure p_m of the explosive blast loading are determined. For thin laminates with the development of membrane forces, a nonlinear theory is required for an accurate output. However, if the pressure is not very high, thick plates can be analyzed quite accurately by a linear theory. The influence of higher modes on the deflection responses is investigated. It was found that contributions from higher modes to deflection responses are quite small. Therefore, a single-mode approach is capable of satisfactory predictions for the response of laminates subject to a sonic boom and an explosive blast.

Appendix: Coefficients of Nonlinear Terms Appearing in Equations (12) and (13)

$$ {}^{U}\bar{S}^{1}_{mnrskl} = \alpha_m \alpha_r^2 S^{1}_{mrk} S^{3}_{nsl} \tag{A1a} $$

$$ {}^{U}\bar{S}^{2}_{mnrskl} = \beta_n \alpha_r \beta_s S^{2}_{mrk} S^{4}_{nsl} \tag{A1b} $$

$$ {}^{U}\bar{S}^{3}_{mnrskl} = \alpha_m \beta_n \beta_s S^{1}_{mrk} S^{4}_{nsl} \tag{A1c} $$

$$ {}^{U}\bar{S}^{4}_{mnrskl} = \alpha_m \beta_s^2 S^{1}_{mrk} S^{3}_{nsl} \tag{A1d} $$

$$ {}^{V}\bar{S}^{1}_{mnrskl} = \alpha_m^2 \beta_s S^{3}_{mrk} S^{2}_{nsl} \tag{A2a} $$

$$ {}^{V}\bar{S}^{2}_{mnrskl} = \alpha_m \alpha_r \beta_s S^{4}_{mrk} S^{2}_{nsl} = {}^{V}\bar{S}^{3}_{mnrskl} \tag{A2b} $$

$$ {}^{V}\bar{S}^{4}_{mnrskl} = \beta_n \beta_s^2 S^{3}_{mrk} S^{1}_{nsl} \tag{A2c} $$

$$ {}^{X}\bar{S}^{1}_{mnrskl} = {}^{V}\bar{S}^{1}_{mnrskl} \tag{A3a} $$

$$ {}^{X}\bar{S}^{2}_{mnrskl} = {}^{V}\bar{S}^{2}_{mnrskl} \tag{A3b} $$

$$ {}^{X}\bar{S}^{3}_{mnrskl} = {}^{V}\bar{S}^{4}_{mnrskl} \tag{A3c} $$

$$ {}^{Y}\bar{S}^{1}_{mnrskl} = {}^{U}\bar{S}^{1}_{mnrskl} \tag{A4a} $$

$$ {}^{Y}\bar{S}^{2}_{mnrskl} = {}^{U}\bar{S}^{2}_{mnrskl} \tag{A4b} $$

$$ {}^{Y}\bar{S}^{3}_{mnrskl} = {}^{U}\bar{S}^{4}_{mnrskl} \tag{A4c} $$

$$ {}^{W}\bar{S}^{1}_{mnrskl} = \alpha_m^2 \alpha_r S^{2}_{mrk} S^{1}_{nsl} + \alpha_m \alpha_r^2 S^{1}_{mrk} S^{1}_{nsl} \tag{A5a} $$

$$ {}^{W}\bar{S}^{2}_{mnrskl} = \alpha_m \beta_n \alpha_r S^{2}_{mrk} S^{1}_{nsl} + \beta_n \alpha_r^2 S^{1}_{mrk} S^{1}_{nsl} \tag{A5b} $$

$$ {}^{W}\bar{S}^{3}_{mnrskl} = {}^{W}\bar{S}^{2}_{mnrskl} \tag{A5c} $$

$$ {}^{W}\bar{S}^{4}_{mnrskl} = {}^{W}\bar{S}^{1}_{mnrskl} \tag{A5d} $$

$$ {}^{W}\bar{S}^{6}_{mnrskl} = \alpha_m \beta_n \beta_s S^{1}_{mrk} S^{2}_{nsl} + \beta_n \alpha_r \beta_s S^{2}_{mrk} S^{2}_{nsl} \tag{A5e} $$

$$ {}^{W}\bar{S}^{7}_{mnrskl} = \alpha_m^2 \beta_s S^{1}_{mrk} S^{2}_{nsl} + \alpha_m \alpha_r \beta_s S^{2}_{mrk} S^{2}_{nsl} \tag{A5f} $$

$$ {}^{W}\bar{S}^{8}_{mnrskl} = {}^{W}\bar{S}^{7}_{mnrskl} \tag{A5g} $$

$$ {}^{W}\bar{S}^{9}_{mnrskl} = {}^{W}\bar{S}^{6}_{mnrskl} \tag{A5h} $$

$$ {}^{W}\bar{S}^{11}_{mnrskl} = \beta_n^2 \alpha_r S^{2}_{mrk} S^{1}_{nsl} + \beta_n \alpha_r \beta_s S^{2}_{mrk} S^{2}_{nsl} \tag{A5i} $$

$$ {}^{W}\bar{S}^{12}_{mnrskl} = \alpha_m \beta_n \alpha_r S^{2}_{mrk} S^{1}_{nsl} + \alpha_m \alpha_r \beta_s S^{2}_{mrk} S^{2}_{nsl} \tag{A5j} $$

$$ {}^{W}\bar{S}^{12}_{mnrskl} = {}^{W}\bar{S}^{13}_{mnrskl} \tag{A5k} $$

$$ {}^{W}\bar{S}^{14}_{mnrskl} = {}^{W}\bar{S}^{11}_{mnrskl} \tag{A5l} $$

$$ {}^{W}\bar{S}^{16}_{mnrskl} = \alpha_m \beta_n \beta_s S^{1}_{mrk} S^{2}_{nsl} + \alpha_m \beta_s^2 S^{1}_{mrk} S^{1}_{nsl} \tag{A5m} $$

$$ {}^{W}\bar{S}^{17}_{mnrskl} = \beta_n^2 \beta_s S^{1}_{mrk} S^{2}_{nsl} + \beta_n \beta_s^2 S^{1}_{mrk} S^{1}_{nsl} \tag{A5n} $$

$$ {}^{W}\bar{S}^{17}_{mnrskl} = {}^{W}\bar{S}^{18}_{mnrskl} \tag{A5o} $$

$$ {}^{W}\bar{S}^{19}_{mnrskl} = {}^{W}\bar{S}^{16}_{mnrskl} \tag{A5p} $$

where

$$ S^{1}_{mrk} = [\lambda(m + r - k) - \lambda(m + r + k) - \lambda(m - r - k) + \lambda(m - r + k)] \tag{A6a} $$

$$ S^{2}_{mrk} = [\lambda(r + m - k) - \lambda(r + m + k) - \lambda(r - m - k) + \lambda(r - m - k)] \tag{A6b} $$

$$ S^{3}_{mrk} = [\lambda(k + r - m) - \lambda(k + r + m) - \lambda(k - r - m) + \lambda(k - r + m)] \tag{A6c} $$

$$ S^{4}_{mrk} = [\lambda(m + r + k) + \lambda(m + r - k) + \lambda(m - r + k) + \lambda(m - r - k)] \tag{A6d} $$

and

$$ {}^{W}\bar{Z}^{1}_{mnrsijkl} = (3/2)\alpha_m \alpha_r \alpha_i^2 Z^{1}_{mrik} Z^{3}_{nsjl} \tag{A7a} $$

$$ {}^{W}\bar{Z}^{2}_{mnrsijkl} = \beta_m \alpha_r \beta_s \alpha_i Z^{2}_{mrik} Z^{1}_{nsjl} + (1/2)\beta_n \beta_s \left(-\alpha_i^2\right) Z^{3}_{mrik} Z^{1}_{nsjl} \tag{A7b} $$

$$ {}^{W}\bar{Z}^{3}_{mnrsijkl} = -\alpha_m^2 \beta_s \beta_j Z^{3}_{mrik} Z^{2}_{nsjl} + \alpha_m \alpha_r \beta_s \beta_j \left(-\alpha_i^2\right) Z^{1}_{mrik} Z^{2}_{nsjl} + \alpha_m \beta_s \alpha_i \beta_j Z^{4}_{mrik} Z^{2}_{nsjl} \tag{A7c} $$

$$ {}^{W}\bar{Z}^{4}_{mnrsijkl} = \alpha_m \beta_n \beta_s \alpha_i Z^{4}_{mrik} Z^{1}_{nsjl} + \alpha_m \alpha_r \left(-\beta_j^2\right)\left(-\alpha_i^2\right) Z^{1}_{mrik} Z^{3}_{nsjl} + \alpha_m \beta_s \alpha_i \beta_j Z^{4}_{mrik} Z^{2}_{nsjl} \tag{A7d} $$

$$ {}^{W}\bar{Z}^{5}_{mnrsijkl} = \alpha_m\alpha_r\beta_s\beta_j Z^{1}_{mrik}Z^{2}_{nsjl} + (1/2)\alpha_m\alpha_r(-\beta_j^2)Z^{1}_{mrik}Z^{3}_{nsjl} \tag{A7e} $$

$$ {}^{W}\bar{Z}^{6}_{mnrsijkl} = (3/2)\beta_n\beta_s\beta_j^2 Z^{3}_{mrik}Z^{1}_{nsjl} \tag{A7f} $$

where

$$ \begin{aligned} Z^{1}_{mrik} = {} & [\lambda(m+r+i-k) + \lambda(m+r-i+k) \\ & - \lambda(m+r+i+k) - \lambda(m+r-i-k) \\ & + \lambda(m-r+i-k) + \lambda(m-r-i+k) \\ & - \lambda(m-r+i+k) - \lambda(m-r-i-k)] \end{aligned} \tag{A8a} $$

$$ \begin{aligned} Z^{2}_{mrik} = {} & [\lambda(i+r+m-k) + \lambda(i+r-m+k) \\ & - \lambda(i+r+m+k) - \lambda(i+r-m-k) \\ & + \lambda(i-r+m-k) + \lambda(i-r-m+k) \\ & - \lambda(i-r+m+k) - \lambda(i-r-m-k)] \end{aligned} \tag{A8b} $$

$$ \begin{aligned} Z^{3}_{mrik} = {} & [\lambda(m-r+i-k) + \lambda(m-r-i+k) \\ & - \lambda(m-r+i+k) - \lambda(m-r-i-k) - \lambda(m+r+i-k) \\ & - \lambda(m+r-i+k) + \lambda(m+r+i+k) \\ & + \lambda(m+r-i-k)] \end{aligned} \tag{A8c} $$

$$ \begin{aligned} Z^{4}_{mrik} = {} & [\lambda(i+m+r-k) + \lambda(i+m-r+k) \\ & - \lambda(i+m+r+k) - \lambda(i+m-r-k) \\ & + \lambda(i-m+r-k) + \lambda(i-m-r+k) \\ & - \lambda(i-m+r+k) - \lambda(i-m-r-k)] \end{aligned} \tag{A8d} $$

where

$$ \lambda(\varphi) = \begin{cases} 1 & \text{if } \varphi = 0 \\ 0 & \text{otherwise} \end{cases} \tag{A9} $$

$$ \varsigma(\varphi) = \begin{cases} [1-(-1)^{\varphi}]/(\varphi\pi) & \text{if } \varphi \neq 0 \\ 0 & \text{otherwise} \end{cases} \tag{A10} $$

References

[1] Niu, M. C-Y., *Composite Airframe Structures Practical Design Information and Data*, Hong Kong Conmilit Press, Hong Kong, 1992.

[2] Reddy, J. N., *Mechanics of Laminated Composite Plates and Shells: Theory and Analysis*, CRC Press, Boca Raton, FL, 2004.

[3] Librescu, L., and Nosier, A., "Response of Laminated Composite Flat Panels to Sonic Boom and Explosive Blast Loadings," *AIAA Journal*, Vol. 28, No. 2, 1990, pp. 345–352.

[4] Librescu, L., Oh, S-Y., and Hohe, J., "Linear and Nonlinear Dynamic Response of Sandwich Panels to Blast Loading," *Composites. Part B, Engineering*, Vol. 35, Nos. 6–8, Sept.–Oct. 2004, pp. 673–683. doi:10.1016/j.compositesb.2003.07.003

[5] Librescu, L., Oh, S-Y., and Hobe, J., "Dynamic Response of Anisotropic Sandwich Flat Panels to Underwater and In-Air Explosions," *International Journal of Solids and Structures*, Vol. 43, No. 13, June 2006, pp. 3794–3816. doi:10.1016/j.ijsolstr.2005.03.052

[6] Hause, T., and Librescu, L., "Dynamic Response of Anisotropic Sandwich Panels to Explosive Pressure Pulses," *International Journal of Impact Engineering*, Vol. 31, No. 5, May 2005, pp. 607–628. doi:10.1016/j.ijimpeng.2004.01.002

[7] Turkmen, H. S., and Mecitoglu, Z., "Nonlinear Structural Response of Laminated Composite Plates Subjected to Blast Loading," *AIAA Journal*, Vol. 37, No. 12, 1999, pp. 1639–1647.

[8] Turkmen, H. S., and Mecitoglu, Z., "Dynamic Response of a Stiffened Laminated Composite Plate Subjected to Blast Load," *Journal of Sound and Vibration*, Vol. 221, No. 3, 1999, pp. 371–389. doi:10.1006/jsvi.1998.1976

[9] Kazanci, Z., and Mecitoglu, Z., "Nonlinear Damped Vibrations of a Laminated Composite Plate Subjected to Blast Load," *AIAA Journal*, Vol. 44, No. 9, 2006, pp. 2002–2008. doi:10.2514/1.17620

[10] Wei, J., and Dharani, L. R., "Response of Laminated Architectural Glazing Subjected to Blast Loading," *International Journal of Impact Engineering*, Vol. 32, No. 12, Dec. 2006, pp. 2032–2047. doi:10.1016/j.ijimpeng.2005.05.012

[11] Gupta, A. D., Gregory, F. H., Bitting, R. L., and Bhattacharya, S., "Dynamic Analysis of an Explosively Loaded Hinged Rectangular Plate," *Computers and Structures*, Vol. 26, Nos. 1–2, 1987, pp. 339–344. doi:10.1016/0045-7949(87)90263-X

[12] Houlston, R., Slater, J. E., Pegg, N., and DesRochers, C. G., "On Analysis of Structural Response of Ship Panels Subjected to Air Blast Loading," *Computers and Structures*, Vol. 21, Nos. 1–2, 1985, pp. 273–289. doi:10.1016/0045-7949(85)90250-0

[13] Houlston, R., and DesRochers, C. G., "Nonlinear Structural Response of Ship Panels Subjected to Air Blast Loading," *Computers and Structures*, Vol. 26, Nos. 1–2, 1987, pp. 1–15. doi:10.1016/0045-7949(87)90232-X

[14] Beshara, F. B. A., "Modeling of Blast Loading on Aboveground Structures, 1. General Phenomenology and External Blast," *Computers and Structures*, Vol. 51, No. 5, 1994, pp. 585–596. doi:10.1016/0045-7949(94)90066-3

[15] Olson, M. D., "Efficient Modeling of Blast Loaded Stiffened Plate and Cylindrical Shell Structures," *Computers and Structures*, Vol. 40, No. 5, 1991, pp. 1139–1149. doi:10.1016/0045-7949(91)90385-Y